Sonophoresis. II. Examination of the Mechanism(s) of Ultrasound-Enhanced Transdermal Drug Delivery

D. Bommannan,[1,5] Gopinathan K. Menon,[2] Hirohisa Okuyama,[3,4] Peter M. Elias,[2] and Richard H. Guy[1,3,6]

Received April 8, 1991; accepted January 26, 1992

We have shown previously that high-frequency ultrasound (sonophoresis) can significantly enhance the transdermal delivery of a topically applied drug *in vivo* and that the augmentation of transport was caused by the action of the ultrasound on the skin. However, these earlier experiments did not reveal (i) the mechanism of sonophoresis, (ii) the pathway of drug permeation under the influence of ultrasound, and (iii) any potentially detrimental effects of the enhancement procedure on skin structure and morphology. In the study reported here, these three key issues have been addressed using electron microscopy to follow the penetration of an electron-dense, colloidal tracer (lanthanum hydroxide; LH). Experiments have again been performed using the hairless guinea pig animal model. Colloidal LH suspensions were applied to skin sites, which were then immediately exposed to ultrasound (at 10 or 16 MHz) for 5 or 20 min. Passive transport of LH under identical conditions (but without ultrasound) provided the control measurements. Tissue processing after the treatment periods utilized standard electron microscopy staining procedures. We found the following: (1) LH does not permeate the skin by passive diffusion; under the influence of ultrasound, on the other hand, it penetrates through the stratum corneum (SC) and the underlying viable epidermal cell layers via an apparently intercellular route. (2) LH transports through the epidermis to the upper dermis, even after only 5 min of ultrasound treatment, a remarkable and unexpected finding. (3) The SC and the cells of the epidermis do not appear to be adversely affected by either (a) ultrasound treatment at 10-MHz frequency (5- or 20-min exposure) or (b) 5 min of sonophoresis at 16 MHz. However, a 20-min treatment with ultrasound at 16 MHz resulted in altered cellular morphology compared to the passive control. The distribution of the tracer in the latter experiments was nonuniform and suggested that cavitational effects may have contributed to the adverse observations. Overall, the results demonstrate that exposure of the skin to ultrasound can induce the considerable and rapid facilitation of LH transport via an intercellular route. Prolonged exposures at high frequencies, however, can alter epidermal morphology, leading us to pose further questions pertaining to the duration and reversibility of ultrasound action on skin.

KEY WORDS: sonophoresis; percutaneous absorption; penetration enhancement; ultrasound; skin barrier function; electron microscopy; lanthanum hydroxide.

INTRODUCTION

In an earlier report (1), we presented evidence that high-frequency ultrasound, at a low intensity (0.2 W/cm^2), can increase transdermal drug flux and decrease percutaneous diffusional lag times. Here, we describe investigations to decipher the mechanism(s) that underlies the observed effects.

Our previous work established that ultrasound acted on the skin, and not on the drug release process from the gel formulation used (1). Here we have used transmission electron microscopy (EM) to track the skin permeation of an electron-dense tracer (colloidal lanthanum). This has allowed us to address (a) the permeation pathway of the diffusing species under the influence of ultrasound, (b) the mechanism of action of ultrasound, and (c) the effects of ultrasound on skin morphology.

The anticipated effects of ultrasound can be broadly classified into two categories: (i) thermal and (ii) nonthermal. Thermal effects are easy to monitor, because they cause an increase in the temperature of the tissue under consideration. In contrast, nonthermal effects are difficult to assess and almost impossible to quantify. We have found that, under the conditions of our experiments, significant skin heating (>1°C) does not occur (1). Theoretical calculations were consistent with these observations (2). Furthermore, the literature reports that temperature changes of more than 5°C are necessary to cause reasonable increases in skin permeability (3,4).

Mechanical and cavitational phenomena constitute the major nonthermal effects due to ultrasound (5). Mechanical effects become significant if the cellular structures are of comparable dimensions to, or larger than, the wavelength of the ultrasound beam. In these circumstances, the cells simultaneously undergo variable stresses and strains leading to mechanical fatigue. However, in the frequency range which we have used (1), the corneocyte dimensions are much smaller than the wavelength of the ultrasound beam. For example, the wavelength of a 10-MHz beam in water is 100 μm, whereas the thickness of a typical corneocyte is of the order of 1 μm. It is highly unlikely, therefore, that the cellular structures of the stratum corneum (SC) (or, indeed, the rest of the skin) are subject to uneven mechanical stresses, which could lead to "fatigue" and cell rupture.

Cavitation is the oscillatory behavior of highly compressible bodies, such as gas, vapor-filled "bubbles," or "cavities" (so-called micronuclei), which are powered by and, therefore, extract energy from the incident acoustic field. Some of this energy (about 10%) is reradiated as an acoustic wave; the remainder, however, is transformed into other forms of energy and may appear as heat (resulting in the production of highly energetic, short-lived chemical species) or as shock waves or hydrodynamic shear fields, which

[1] Graduate Group in Bioengineering, University of California, Berkeley, and University of California, San Francisco, California 94143.

[2] Department of Dermatology, University of California, San Francisco, California 94143, and VA Medical Center, 4150 Clement Street, San Francisco, California 94121.

[3] Departments of Pharmacy and Pharmaceutical Chemistry, University of California, San Francisco, California 94143.

[4] SS Pharmaceutical Co., Inc., Tokyo, Japan.

[5] Current address: Cygnus Therapeutic Systems, Redwood City, California 94063.

[6] To whom correspondence should be addressed at Departments of Pharmacy and Pharmaceutical Chemistry, University of California, San Francisco, California 94143.

0724-8741/92/0800-1043$06.50/0

can easily disrupt biological tissues. The occurrence of cavitation in a medium is crucially dependent upon the number and availability of these micronuclei, the intensity and frequency of the ultrasound wave, and a number of additional variables. Furthermore, cavitation occurs randomly and is, therefore, more difficult to study. There are a few *in vitro* studies which report the effects of ultrasound in the megahertz range on human platelets. Miller *et al.* (6,7), for example, showed that these cells aggregate when exposed to ultrasound at intensities <100 mW/cm^2. However, the cavitational effects on skin caused by high-frequency ultrasound have not been examined. Even in the case of diagnostic ultrasound, which has been used for decades, the possible adverse effects of cavitation remain unclear (8). To our knowledge, we present here the first examination of nonthermal (cavitational) effects caused by high-frequency ultrasound on skin *in vivo*.

MATERIALS AND METHODS

Adult hairless guinea pigs (Charles River Laboratories, Boston, MA) were anesthetized with ketamine (approximately 500 mg/kg; QUAD Pharmaceuticals, Indianapolis, IN). An aqueous suspension of colloidal lanthanum hydroxide (LH) was prepared by dissolving lanthanum nitrate (2%, w/v) in water, and the pH of the solution was adjusted to 7.6 by the addition of sodium hydroxide. The suspension was applied topically to one of the animal's flanks; the site was then immediately treated with 10- or 16-MHz ultrasound (at 0.2 W/cm^2) for either 5 or 20 min. The ultrasound equipment and its validation were the same as those described in our earlier publication (1). The LH suspension was an adequate ultrasound coupling medium, and the penetrated lanthanum served as an electron dense tracer for microscopic visualization (9). Unlike the permeation experiments (1), in which control and treatment procedures were performed on the same animal to minimize intersubject variability, the EM work utilized different animals in the two sets of experiments because of the invasive nature of the protocol. As before (1), control experiments were identical to those outlined here except that the transducer was not activated. After the exposure period, full-thickness skin was biopsied using a 5-mm punch. The excised skin was then carefully cut into smaller pieces (<0.5 mm), which were fixed in modified Karnovsky's fixative for 1 hr at room temperature and then left overnight at 4°C. Subsequently, the samples were rinsed with cacodylate buffer (0.1 *M*, pH 7.3), postfixed in buffered ice-cold 1% OsO_4 for 1 hr, dehydrated in graded ethanol solutions, and embedded in an Epon–epoxy mixture (9). Thin sections (600–800 nm), cut using an MT2B ultra microtome, were examined either unstained or after double staining with uranyl acetate and lead citrate, using a Zeiss electron microscope (Model 10A; Carl Zeiss, Inc., Thornwood, NY) operated at 60 kV.

RESULTS

Controls

Control preparations, to which LH was applied topically without activating the ultrasound transducer, showed normal epidermal morphology and a compact SC, with the secreted contents of lamellar bodies filling the intercellular domain at the stratum granulosum (SG)–stratum corneum (SC) junction (Fig. 1). There was no evidence of tracer permeation into the intercellular domains of SC (Fig. 2) or extending into the nucleated cell layers below (SG). Basal cells displayed abundant ribosomes, mitochondria (M), keratin filaments (KF), and hemidesmosomes (HD) at the zone of contact with the basement membrane (BM). Intercellular spaces are prominent between the adjacent cells of stratum basale (Fig. 4). Superficial dermis shows collagen filaments (C) in both longitudinal and cross-sectional profile and is devoid of any tracer particles (Fig. 4). These studies indicate that the tracer neither penetrates into nor traverses the intact permeability barrier.

Ultrasound-Treated Skin

Pathways and Extent of Penetration. In animals treated with ultrasound for 5 min, LH appeared patchily distributed within the intercellular domains of the SC (Fig. 3). Abundant precipitates of the tracer were found in (a) the intercellular spaces of the stratum basale (SB), (b) the zona lucida of the basement membrane region, and (c) in the superficial dermis (Figs. 5–8). The lower dose of ultrasound (10 MHz for 5 min) also drove LH into the dermis (Fig. 6), and as with the higher dose, the tracer again concentrated at the epidermal–dermal junction. These micrographs provide strong evidence that the epicutaneously applied tracer permeated through the intercellular route. In comparison to the discrete distribution of LH after ultrasound treatment for 5 min, the longer period (20 min) of sonophoresis led to more extensive accumulation and aggregation of the tracer within the dermis (Figs. 9 and 10).

Morphological Effects. The morphology of nucleated

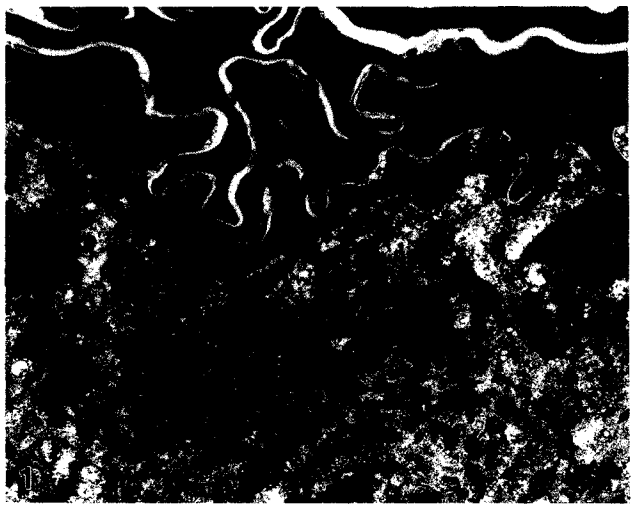

Fig. 1. Electron micrograph of control skin not previously exposed to ultrasound. Shown are outer layers of the epidermis, the stratum corneum (SC), and the stratum granulosum (SG) cells below the SC–SG junction. In the SC, the dark structures are the corneocytes and the electron-lucent regions are the lipid-enriched intercellular domains between the corneocytes. Keratohyalin (kh) appears as dark patches in the outer SG. Arrows point to secreted lamellar body contents at the SC–SG junction. n, nucleus. ×16,000; reduced to 65% for reproduction.

Fig. 2. Electron micrograph of control SC demonstrating the absence of tracer in both cytosolic and intercellular (⋆) domains. ×32,000; reduced to 69% for reproduction.

Fig. 4. Electron micrograph of control skin showing the basal layer, epidermal–dermal junction, basement membrane (bm), and dermis (D). The collagen fibers are arranged in bundles, which are seen as rods in longitudinal section and as circles in cross section. Note the complete absence of tracer between adjacent basal cells and in the dermis. kf, keratin filaments; m, mitochondria; hd, hemidesmosomes. ×24,000; reduced to 65% for reproduction.

epidermal cells was not apparently altered by 5 min of exposure to ultrasound (Figs. 5–8). However, 20 min of sonophoresis damaged some of these cells (Fig. 12). In contrast, the cytosol and membranes of the corneocytes were unaffected and looked similar in appearance to the untreated controls (Fig. 11).

DISCUSSION

The results presented above demonstrate unequivocally that low-intensity sonophoresis rapidly drives a hydrophilic, colloidal tracer across the epidermal permeability barrier into the dermis. While the relevance of LH transport to the diffusion of lipophilic drugs, for example, can be questioned, the usefulness of the approach for (a) direct visualization of permeation pathways and (b) determination of the time course of such a delivery mechanism is clear. Confocal microscopy is another promising method for the visualization of transport pathways, but it is expensive, is limited to certain classes of nonreactive fluorophores, and awaits complete validation by complementary methods (10). Soluble-tracer autoradiography, at the light microscopic level, has been used (11), but the approach is technically demanding and does not provide sufficient resolution to allow evaluation of toxicity in the same sample. Another method of potential interest is *in situ* precipitation, which depends on the generation of an electron-dense reaction product within the stratum corneum (12,13).

Lanthanum nitrate solution, at a pH slightly greater than 7, generates a suspension of lanthanum hydroxide particles (14), which are the smallest colloidal tracers known (15). Penetration of this probe through membrane junctions has, therefore, been used to evaluate the integrity of permeability barriers in a variety of tissues (16). A most unexpected result in the present study was the appearance of tracer at all levels of the epidermis, and in the dermis, after only 5 min of sonophoresis at 16 MHz. Since LH permeation by passive diffusion in the control experiments was not measurable, it can be assumed that sonophoresis was responsible for the observed tracer displacement. In parallel studies, utilizing an alternative penetration enhancement technique, we have found that continuous iontophoresis for 45 min drove the tracer only to the level of the stratum granulosum of hairless mouse skin (unpublished observations). Therefore, the finding that sonophoresis, for a period as short as 5 min, can deliver

Fig. 3. Electron micrograph of SC after 5 min of ultrasound treatment at 16-MHz frequency showing the patchy distribution of the tracer (arrows) in the intercellular spaces of the SC. ×20,000; reduced to 69% for reproduction.

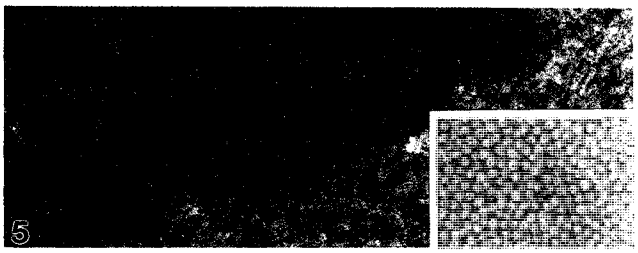

Fig. 5. Electron micrograph of skin after treatment with ultrasound for 5 min at a 16-MHz frequency showing the lanthanum tracer as discrete electron-dense particles (i) between a basal cell (stratum basale; SB) and the basement membrane (bm) zone and (ii) within the dermis (D). ×20,000; Inset: Lanthanum deposition around collagen bundles (compare with Fig. 4). ×28,000; reduced to 65% for reproduction.

Fig. 6. Electron micrograph of skin treated for 5 min with 10-MHz ultrasound. The tracer has been driven deep into the dermis (D). However, lanthanum (arrows) is less abundant than that observed after 16-MHz treatment for an equivalent period. ×20,000; reduced to 65% for reproduction.

tracer into dermal tissues provides new support for the potential of this approach in percutaneous drug delivery.

Electron microscopy reveals further details about the possible paths of tracer penetration across the SC. Within the SC, the tracer appears to be patchily distributed within the intercellular lipid lamellae within the locales that correspond to the "lacunae" that punctuate the lipid bilayers (17), previously suggested to be possible polar or head-group domains. The possibility that these channels may be interconnected, serving as a tortuous reticulum of hydrophilic domains, needs to be examined. Once past the SC, the tracer seems to be uniformly distributed within the hydrophilic intercellular spaces of the nucleated layers of the epidermis. However, it is also possible that 5 min of sonophoresis drove most of the tracer through the outer epidermal layers, and down to the SB, and therefore the tracer may have been "chased" through by sonophoresis.

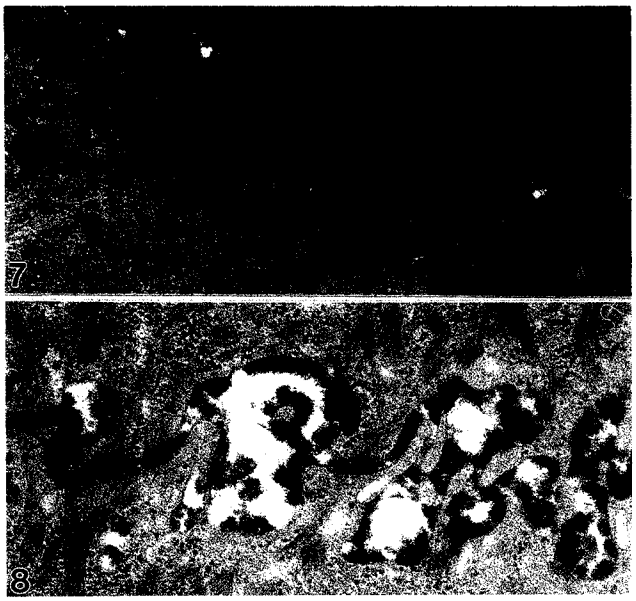

Figs. 7 and 8. Electron micrographs of skin after 5-min treatment at 16-MHz frequency, indicating that, even within this short time, the tracer (arrows) has traversed the stratum corneum and most of the epidermis, to the stratum basale (SB) (Fig. 7). Figure 8 shows abundant tracer in the intercellular spaces of the SB. Fig. 7, ×13,600; Fig. 8, ×30,000; reduced to 69% for reproduction.

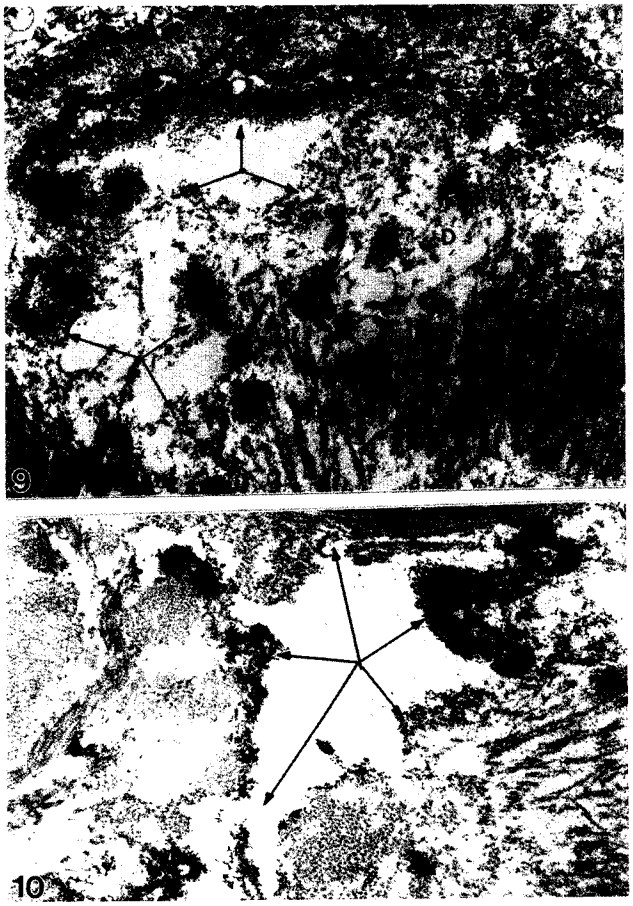

Figs. 9 and 10. Electron micrographs showing the presence of the tracer in large aggregates in the dermis (D) and subjacent to the basement membrane (bm) after 20 min of ultrasound at 16-MHz frequency. Arrows indicate possible cavitational effects (see text). Fig. 9, ×10,000; Fig. 10, ×10,000; reduced to 65% for reproduction.

Finally, the effects of ultrasound on the cellular structures of the skin require comment. Sonophoresis for 5 min, at either 10 or 16 MHz, did not appear to alter cellular morphology. However, 20 min of sonophoresis at 16 MHz appeared to result in significant cytotoxic effects. Cavitation may have produced this adverse finding. This suggestion is based on Figs. 9 and 10, in which the tracer appears to be aggregated and to line the surface of imaginary spheres (compared to the discrete distribution of particles seen in Figs. 5 to 8). The aggregation of tracer following the extended treatment at 16 MHz could be explained by the following mechanism. Assume the presence of bubbles (micronuclei) in the intercellular spaces. It is plausible that 20 min of continuous-wave ultrasound causes this bubble to grow (cavitation). The tracer in this region that is initially dispersed can now be pushed toward adjoining cell structures by bubble expansion. Finally, when the bubble collapses, the tracer may be in close proximity to the surface of the adjacent structures (as suggested by Figs. 9 and 10). Concomitantly, the repeated expansion and self-destruction of micronuclei in the skin due to cavitation may induce enhanced penetration of the permeant. We believe that Fig. 10 provides evidence that cavitation occurs. We refrain, at this

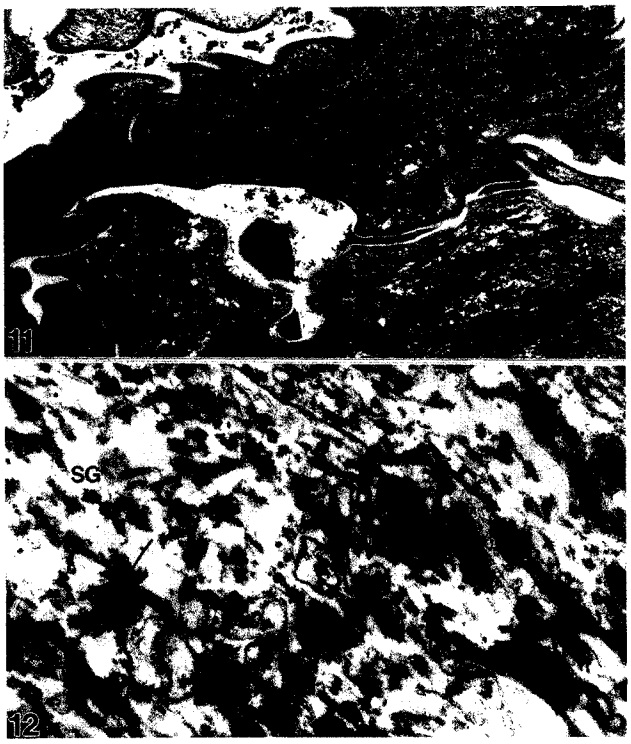

Figs. 11 and 12. Electron micrographs of epidermis after 20-min treatment with 16-MHz ultrasound at 0.2-W/cm^2 intensity. Compare the normal-appearing stratum corneum (SC) (Fig. 11) with the cytotoxicity within the stratum granulosum (SG) cells (Fig. 12). Again, tracer is observed primarily between the cells (arrows), even in the presence of extensive cytotoxicity. Fig. 11, ×30,000; Fig. 12, ×40,000; reduced to 65% for reproduction.

time, from characterizing the effect as either stable or unstable cavitation—both phenomena could produce the observed effects, but our "detection" technique (i.e., EM) cannot distinguish between the two. While stable and unstable cavitations exhibit different kinds of bubble behavior in response to an acoustic field, violent stable cavitation is not easily differentiated from unstable cavitation.

In summary, this investigation has examined the effects of ultrasound on the permeation of an electron-dense tracer. The results reveal that 5 min of sonophoresis, at a frequency of 10 or 16 MHz, delivers the tracer through the epidermis into the dermis, a remarkable achievement. The penetration pathway of the tracer appears to be intercellular. Longer exposure of the skin to high-frequency ultrasound (20 min, 16 MHz) resulted in structural alterations of the stratum granulosum and stratum basale cells. These results lead us to questions of reversibility and the adverse effects of different frequencies and exposure times. Are the changes induced by ultrasound irreversible? If they are, how long does the perturbation last? These issues remain unanswered and must form the basis of future work.

ACKNOWLEDGMENTS

This research was supported by Grants HD-23010 and AR-19098 from the U.S. National Institutes of Health, by the Veterans Administration, and by Cygnus Therapeutic Systems. D.B. was the recipient of a Graduate Student Research Award from UCSF.

REFERENCES

1. D. Bommannan, H. Okuyama, P. Stauffer, and R. H. Guy. Sonophoresis. I. The use of ultrasound to enhance transdermal drug delivery. *Pharm. Res.* 9:559–564 (1992).
2. D. Bommannan. Ph.D. thesis, University of California, San Francisco.
3. R. O. Potts and M. L. Francoeur. Lipid biophysics of water loss through the skin. *Proc. Natl. Acad. Sci.* 87:3871–3873 (1990).
4. K. Knutson, R. O. Potts, D. B. Guzek, G. M. Golden, J. E. McKie, W. J. Lambert, and W. I. Higuchi. Macro- and molecular physical-chemical considerations in understanding drug transport in the stratum corneum. *J. Control. Release* 2:67–87 (1986).
5. A. R. Williams. *Ultrasound: Biological Effects and Potential Hazards,* Academic Press, San Francisco, 1983.
6. M. W. Miller, G. E. Kaufman, F. L. Cataldo, and E. L. Cartensen. Absence of mitotic reduction in regenerating rat livers exposed to ultrasound. *J. Clin. Ultrasound* 4:169–172 (1976).
7. D. L. Miller, W. L. Nyborg, and C. C. Whitcomb. Platelet aggregation induced by ultrasound under specialized conditions in vitro. *Science* 205:505–507 (1979).
8. American Institute of Ultrasound in Medicine. Bioeffects report. *J. Ultrasound Med.* 7:S1–S38 (1988).
9. P. M. Elias and B. E. Brown. The mammalian cutaneous permeability barrier. *Lab. Invest.* 39:574–583 (1987).
10. C. Cullander, G. K. Menon, R. H. Guy, and P. M. Elias. In situ visualization of the lamellar body secretory system by confocal microscopy. *J. Invest. Dermatol.* 94:517 (1990).
11. H. Schaefer, G. Stuttgen, A. Zesch, W. Schalla, and J. Gazith. Quantitative determination of percutaneous absorption of radiolabeled drugs in vitro and in vivo by human skin. *Curr. Problems Dermatol.* 7:80–94 (1978).
12. H. E. Boddé, M. A. Kruithof, J. Brussee, and H. K. Koerten. Visualization of normal and enhanced $HgCl_2$ transport through human skin *in vitro*. *Int. J. Pharm.* 53:13–24 (1989).
13. M. K. Nemanic and P. M. Elias. In situ precipitation: A novel cytochemical technique for visualization of permeability pathways in mammalian stratum corneum. *J. Histochem. Cytochem.* 28:573–578 (1980).
14. J. P. Revel and M. J. Karnovsky. Hexagonal array of subunits in intercellular junctions of the mouse heart and liver. *J. Cell Biol.* 33:C7–C12 (1967).
15. M. A. Hayat. *Positive Staining for Electron Microscopy,* Van Nostrand Reinhold, New York, 1975, pp. 163–186.
16. I. S. Harper, K. Williams, and A. Lochner. Lanthanum probing of cell membrane permeability in the rat heart: Pathological versus artefactual alterations. *J. Electron Microsc. Tech.* 14:357–366 (1990).
17. S. E. Hou, A. K. Mitra, S. H. White, G. K. Menon, R. Ghadially, and P. M. Elias. Membrane structures in normal and essential fatty acid-deficient stratum corneum: Characterization by ruthenium tetroxide staining and X-ray diffraction. *J. Invest. Dermatol.* 96:215–223 (1991).